Dalton
www.rsc.org/dalton

Outer sphere anion participation can modify the mechanism for conformer interconversion in Pd pincer complexes

John R. Miecznikowski,[a] Stephan Gründemann,[a] Martin Albrecht,[a] Claire Mégret,[b] Eric Clot,[b] Jack W. Faller,*[a] Odile Eisenstein*[b] and Robert H. Crabtree*[a]

[a] *Department of Chemistry, 225 Prospect Street, Yale University, New Haven CT 06520-8107, USA. E-mail: robert.crabtree@yale.edu; jack.faller@yale.edu*

[b] *LSDSMS (UMR 5636), cc14, Université Montpellier 2, 34095 Montpellier Cedex 05, France. E-mail: odile.eisenstein@univ-montp2.fr; clot@univ-montp2.fr*

Received 1st November 2002, Accepted 18th December 2002
First published as an Advance Article on the web 29th January 2003

Interconversion of the two chiral conformations of the square planar Pd(II) CCC pincer carbene complex, **1** (η^3-*C*,*C*′,*C*″) (2,6-bis{[*N*-methyl-*N*′-methylene]imidazol-2-ylidene}phenyl)bromopalladium(II), and the CNC cation, **2**, (η^3-*C*,*C*′,*N*)(2,6-bis{[*N*-methyl-*N*′-methylene]imidazol-2-ylidene}pyridine)bromopalladium(II)(1+), is characterized by VT NMR spectroscopy. Combined DFT/experimental work indicates two alternative mechanisms. In the case of **1**, having no counterion, and several derivatives of **2** with weakly nucleophilic counterions, the fluxional process goes in two steps *via* an unsymmetrical cationic 4-coordinate intermediate. In this case one carbene ring moves through the square plane before the other. In some cases for **2** with more nucleophilic counterions, such as [{CNC}PdI]I, a second lower-barrier process takes over that depends on the nature of the counterion. We propose that the outer sphere anion reversibly displaces the central N (pyridine) unit of the pincer in a rate limiting step to form a neutral dihalo intermediate that undergoes rapid conformer interconversion. This accounts for the counterion dependence and constitutes an unusual type of fluxionality that couples anion substitution at the metal with the conformational change of the ligand. A pyridine, even when present as the central element of a CNC pincer ligand, can therefore be labile even under mild conditions and reaction mechanisms involving decoordination of such group are therefore possible.

Introduction

We recently reported[1] the Pd CCC (CCC = (η^3-*C*,*C*′,*C*″) (2,6-bis{[*N*-methyl-*N*′-methylene]imidazol-2-ylidene}phenyl)) and CNC (CNC = (η^3-*C*,*C*′,*N*)(2,6-bis{[*N*-methyl-*N*′-methylene]-imidazol-2-ylidene}pyridine)) pincer complexes, **1** {CCC}-Pd(X_{IS}), and salts **2**, [{CNC}Pd(X_{IS})][X_{OS}], where the two possible twisted chiral conformations (eqns. 1 and 2) interconvert on the NMR timescale and where X_{IS} and X_{OS} refer to the inner sphere and outer sphere anions respectively. The interconversion is potentially relevant for asymmetric catalysis,[2] where it would need to be prevented. Others have reported similar complexes.[3] Experimental and DFT studies, reported here, suggest a pathway in which the two methyl groups successively pass through the plane of the complex but without a planar structure as intermediate.

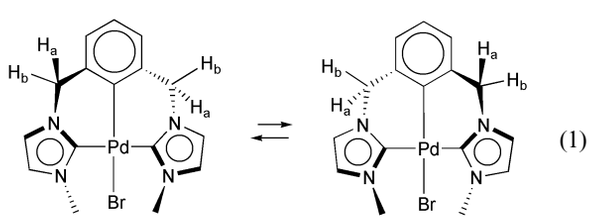

1 **1'** (1)

Studies on **2** reveal an unexpected dependence of the fluxional rate on the nature of the counter ion. Experimental and DFT studies now suggest that nucleophilic outer sphere anions can in certain cases displace the pyridine moiety of the CNC pincer in **2** to give a lower-barrier path for fluxionality than that for **1**, and for other salts of **2** having weakly nucleophilic counterions, where such decoordination cannot or does not occur. The second pathway is unusual because in the common forms of fluxionality,[4] a metal complex only changes the ligand conformation or the geometry around the metal but the coordination sphere remains unchanged.[5]

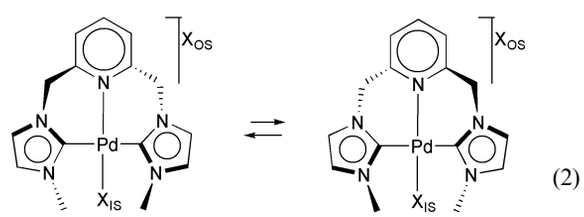

2 **2'** (2)

(X_{IS} = X_{OS} = Cl, Br, I)

(X_{IS} = Cl, Br, I; X_{OS} = OTs)

Results and discussion

Synthesis

The synthesis of **1** and **2** (X_{IS} = X_{OS} = Br) has been described,[1] and the preparations of **2** (X_{IS} = X_{OS} = Cl) are reported in this paper. Other derivatives of **2** shown in Table 1 were prepared by anion exchange. In particular, the known complexes **2** (X_{IS} = X_{OS} = Cl or Br) react with $AgBF_4$ to give an intermediate aqua complex, [{CNC}Pd(OH_2)][BF_4]$_2$, which in turn reacts with excess NaI in acetone for 16 h to give **2** (X_{IS} = X_{OS} = I). The chloro species, **2**, (X_{IS} = X_{OS} = Cl) was treated with 1 equiv. NaOTs in CH_2Cl_2 for 48 h to give the tosylate **2** (X_{IS} = Cl; X_{OS} = OTs). AgOTs was needed instead of NaOTs to give the tosylate for the bromide and iodide, **2** (X_{IS} = Br, I; X_{OS} = OTs). A crystallographically useful sample of [{CNC}Pd(OH_2)][BF_4]$_2$ was not obtained, but addition of pyridine gave [{CNC}Pd-(C_5H_5N)][BF_4]$_2$, for which a crystal structure was obtained.

NMR studies

Variable temperature ^{1}H NMR studies have been carried out in the solvents shown in Table 1. The two types of CH_2 proton in the methylene linker, H_a and H_b, occur as a mutually coupled pair of signals at low temperature, but on warming coalesce

DOI: 10.1039/b210784h

Table 1 Data on the fluxionality

Entry	Complex	T(coal.)/K	$\Delta G^{\dagger}$/kJ mol^{-1}	Solvent
1	[{CCC}PdBr]	350	70.9	d_6-dmso
2	[{CNC}PdCl]Cl	308	59.3	$CDCl_3$
3	[{CNC}PdCl]OTs	343	66.0	d_6-dmso
4	[{CNC}PdBr]Br	278	52.9	$CDCl_3$
5	[{CNC}PdBr]OTs	373	77.6	d_6-dmso
6	[{CNC}PdI]I	208	41.9	CD_2Cl_2
7	[{CNC}PdI]OTs[a]	338	70.9	d_6-dmso
8	[{CNC}Pd(OH_2)][BF_4]$_2$	>353	>73	$CDCl_3$
9	[{CNC}PdCl]Cl	303	60.0	CD_2Cl_2
10	[{CNC}Pd(py)][BF_4]$_2$	>403	>73	d_6-dmso
11	[{CNC′}PdBr]Br	303	57.4	$CDCl_3$
12	[{CNC}Pd(OH_2)][BF_4]$_2$	343	68.5	d_6-dmso

[a] This compound could never be obtained pure and always had an I : Pd ratio >1.

because they exchange environments during the fluxional process (eqns. 1 and 2). Lineshape analysis or the line-broadening method described by Faller allowed the rate of the fluxional process to be extracted (Table 1) as discussed previously.[1,6,7]

The simplest situation exists for **1** (Table 1, entry 1), where there is a bound halide only. As a neutral complex, **1** has no outer sphere counter ion, X_{OS}. We did not attempt to vary the bound halide in the synthesis. We did vary X in the calculations of the CCC complex and saw no significant difference in the transition state barrier when the halide was varied.

The case of **2** proved more interesting. Where $X_{IS} = X_{OS} = Br$, the fluxional process for **2** had a far lower barrier than for **1** (entry 4). Since we have found many cases where counterions play a large role in the chemistry,[8–10] we decided to look at the effect of changing the X_{OS} ion from Br to the weakly nucleophilic OTs. The barrier was greatly enhanced (entry 5) and exceeded that seen earlier for **1**. The barrier enhancement on changing $X_{IS} = X_{OS}$ = halide to X_{IS} = halide, X_{OS} = OTs was greatest for the iodide case (entries 6–7), where it increased from 42 to 71 kJ.mol^{-1}. Conversely, for chloride the change was rather modest (entries 2–3). Iodide, showing the greatest effect and being the softest nucleophile, suggested the possibility that it might attack the metal most rapidly in the fluxional process. The solvent, CD_2Cl_2, which has a low freezing point, was needed for the study on **2** ($X_{IS} = X_{OS}$ = I), but for other cases such as [{CNC}PdCl]Cl we verified that the change of solvent gave a small change of barrier. As reported[1] earlier for [{CCC}PdBr] and [{CNC}PdBr]Br, the rates are independent of solvent ($CDCl_3$ *vs.* d_6-dmso) so the ion pairing discussed in this paper seems to be retained in both solvents. However, the solvent did affect $\Delta G^{\dagger}$ for the [{CNC}Pd(OH_2)][BF_4]$_2$ complex (entries 8 and 12), so in this case the DMSO may well displace the water and act as a ligand.

We used 30 mole equivalents of excess halide to probe the possibility of outer sphere halide attacking the complex, but instead of the expected barrier decrease, a slight increase was seen. The absence of the expected effect is ascribed to the presence of tight ion pairs[11] in solution making the fluxional process effectively intramolecular. The change in the presence of excess halide is probably a salt effect by which the polarity of the solvent is increased, favouring the ion pair form over the neutral intermediate (see below).

Replacement of all the halides by the weakly nucleophilic anion BF_4 proved possible. The resulting aqua compound, formed from adventitious water, gave a high barrier (entries 8 and 12) reminiscent of **1**. Replacement of the aqua group by pyridine to give the crystallographically characterized pyridine complex resulted in a very large increase in the barrier (entry 10). For this study, high boiling d_6-dmso had to be used as solvent. No coalescence was observed and hence a $\Delta G^{\dagger}$ value could not be determined for the pyridine complex.

The barrier was somewhat sensitive to the nature of the wingtip group, R. This was methyl in all the cases described above, denoted by CNC in the formulae, but in one case we used n-Bu wingtips, denoted by CNC′. Comparison of entries 4 (R = Me) and 11 (R = n-Bu) show that the increased steric hindrance of the larger R group leads to a 4.5 kJ mol^{-1} increase in the barrier height.

Crystallographic study

To verify the solid state structure in one case, crystals of [{CNC}Pd(py)][BF_4]$_2$ were grown by slow diffusion of Et_2O into a methanol solution of [{CNC}Pd(py)][BF_4]$_2$ and studied crystallographically (Fig. 1 and Tables 2 and 3).

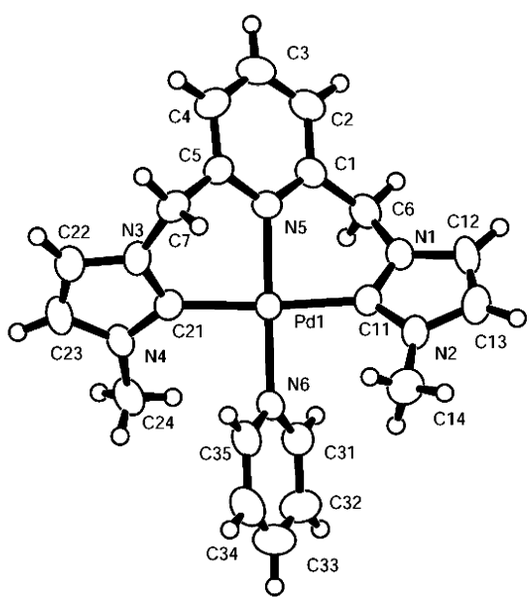

Fig. 1 X-Ray structure of the pyridine complex.

The structure of [{CNC}Pd(py)][BF_4]$_2$ resembles that previously described[1] for **1** (X_{IS} = Br) and **2** ($X_{IS} = X_{OS}$ = Br). For **1** and **2**, the single crystal structure analyses showed that the ligands are strongly puckered.[1] The dihedral angle, C(1)–C(6)–Pd(1)–C(11), in **1** was 42.9(7)° *versus* the corresponding angle C(1)–N(5)–Pd(1)–C(11) in **2** of 40.4(4)°.[1] In addition, the Pd–C(6), **1**, and Pd–N(5), **2**, bond lengths were virtually identical.[1] But, the different *trans* influence of pyridine *vs.* the aryl is shown by the difference in the Pd–Br bond distances *trans* to the aryl C(6) (2.5388(10) Å in **1**) *vs. trans* to the pyridine N(5) (2.4250(5) Å in **2**).[1]

The chelate in [(CNC)Pd(py)][BF_4]$_2$ has bite angles slightly less than 90°. All of the rings are twisted out of the square plane of the metal and its donor atoms. This is shown by the dihedral angles N(5)–Pd(1)–C(11)–N(1) = −35.5(3)° and N(5)–Pd(1)–C(21)–N(3) = 40.3(4)°. These angles would be 0° if the

Table 2 Selected bond lengths and angles for complex [{CNC}-Pd(C_5H_4N)][BF_4]$_2$

Bond lengths/Å	
Pd(1)–N(5)	2.060(4)
Pd(1)–N(6)	2.017(4)
Pd(1)–C(11)	2.021(4)
Pd(1)–C(21)	2.027(4)
Bond angles/deg.	
N(5)–Pd(1)–C(11)	87.8(2)
N(5)–Pd(1)–C(21)	88.4(2)
N(6)–Pd(1)–C(11)	92.1(2)
N(6)–Pd(1)–C(21)	91.8(2)
N(5)–Pd(1)–N(6)	178.5(2)
C(11)–Pd(1)–C(21)	175.6(2)
Dihedral angles/deg.	
C(11)–Pd(1)–N(5)–C(1)	−41.1(3)
C(11)–Pd(1)–N(6)–C(1)	−65.1(3)
N(6)–Pd(1)–C(11)–N(2)	40.4(4)
N(6)–Pd(1)–C(21)–N(4)	39.2(5)

Table 3 Crystal data and structure refinement for [{CNC}-Pd(C_5H_4N)][BF_4]$_2$

Formula	$C_{20}H_{22}B_2F_8N_6Pd$
Formula weight	626.44
Crystal dimensions/mm	0.07 × 0.07 × 0.12
Crystal system	triclinic
Space group	$P\bar{1}$
a/Å	9.8872(5)
b/Å	9.9387(5)
c/Å	12.7418(6)
α/°	77.790(3)
β/°	86.260(3)
γ/°	85.324(3)
V/Å^3	1218.2(1)
Z	2
F(000)	624.00
T/K	183.2
D_c/Mg m^{-3}	1.708
μ(Mo-Kα)/mm^{-1}	0.845
No. collected reflections	15462
No. unique reflections, R_{int}	5578, 0.047
No. of observed reflections	3701
No. of refined parameters	334
$wR(F)$	0.049
$R[I > 3\sigma(I)]$	0.041
Goodness-of-fit	1.18
($\Delta\rho$) max, min/e Å^{-3}	0.92, −0.50

imidazole rings lay in the plane and ±90° if they were normal to the plane. The pyridine rings have torsion angles of C(11)–Pd(1)–N(5)–C(1) = −41.1(3)° and C(11)–Pd(1)–N(6)–C(31) = −65.1(3)°. The chelated pyridine and carbenes are more than 45° from the normal to the square plane. The unchelated pyridine is twisted ~25° from the normal to the square plane, which presumably arises from interactions with the methyl groups. The constraints of tridentate chelation lengthen the bond to the chelated pyridine N (Pd(1)–N(5): 2.060(4) Å), *versus* the unchelated one (Pd(1)–N(6) 2.017(4) Å).

Computational studies

DFT(B3PW91) calculations were carried out to gain some insight into the difference in fluxionality of systems **1** and **2**. The whole pincer including the two methyl groups has been introduced in the calculated systems. To test the quality of our computational strategy we compared the optimized geometry of Pd{CCC}Br, **GS(1Br)**, and Pd{CNC}Br, **GS(2Br)**, with the X-ray structures of complexes **1** (X_{IS} = Br) and **2** (X_{IS} = Br and X_{OS} = Br).[1] The calculated C_2 geometry of the reactants, **GS(1Br)** and **GS(2Br)**, is very well reproduced (Fig. 2 and Table 4). The twist of the pincer almost allows Pd to attain a square planar geometry (C(11)–Pd–C(21) = 172.2°, C(6)–Pd–Br = 180°, **GS(1Br)**; C(11)–Pd–C(21) = 174.9°, N(5)–Pd–Br = 180°, **GS(2Br)**). The methyl group is significantly out of the molecular plane defined by the pincer carbons as indicated by the dihedral angles (C(1)–C(6)–Pd–C(11) = 41.3°, **GS(1Br)**; C(1)–N(5)–Pd–C(11) = 41.0°) which are very close to the experimental values (42.9° and 40.6°, respectively). The numbering scheme of Fig. 2 will be used to describe all subsequent calculations.

Table 4 Comparison of experimental[1] bond distances and angles for Pd{CEC}Br, **1** (E = C), and [Pd{CEC}Br][Br], **2** (E = N), with that of the calculated complexes Pd{CEC}Br, **GS(1Br)** (E = C), and Pd{CEC}Br$^+$,**GS(2Br)** (E = N)

	1	**GS(1Br)**	**2**	**GS(2Br)**
Bond lengths/Å				
Pd–E	2.014	2.017	2.066	2.093
Pd–C(11)	2.00	2.035	2.020	2.034
Pd–Br	2.5388	2.558	2.4250	2.422
C(12)–C(13)	1.33	1.366	1.328	1.358
Bond angles/deg.				
C(11)–Pd–C(21)	170.9	172.2	173.2	174.9
E–Pd–C(11)	85.1	86.1	86.7	87.5
E–Pd–Br	179.6	180.0	178.9	180.0
Dihedral angles/deg.				
C(1)–E–Pd–C(11)	42.9	41.3	40.6	41.0
N(1)–C(7)–C(1)–C(6)	49.3	52.7	57.2	56.3
N(2)–C(11)–C(21)–N(4)	95.4	96.8	101.3	91.8

a) The {CCC}Pd(X_{IS}) systems. The mechanism of the fluxional process for {CCC}Pd(X_{IS}) has been studied for X_{IS} = Cl, Br and I. The calculations show that the two wingtip methyl groups of the carbene ligands are never simultaneously in the plane defined by the pincer and the metal, a location that would be very sterically unfavourable. The fluxionality thus proceeds in a two-step process with one methyl at a time crossing the molecular plane (Fig. 3). The facile distortion possible in d^8 ML_4 allows additional relief of the steric repulsion during the fluxional process.[12] With these two aspects in mind we now proceed to describe the path for X = Br, a complex having a known structure.[1] The transition state **TS(1Br)** brings one methyl, on N(4), into the molecular plane (Fig. 3, see Fig. 2 for atom numbering). This is accompanied by a significant elongation of both Pd–C(6) (+0.031 Å) and Pd–C(21) (+0.032 Å) *trans* and *cis* to Br, respectively. The other angles adjust with a slight opening of the C(6)–Pd–C(21) and C(21)–Pd–Br angles. The other methyl group moves slightly away from the molecular plane C(6)–Pd–C(11)–N(2) = 139.2°. The coordination of the Pd is no longer strictly square planar: the C(11)–Pd–C(21) decreases and the bromide is not *trans* to C(6) (Table 5). These structural changes prevent the *N*-methyl group coming too close to Pd (non-bonded distances: Pd ··· C(14) = Pd ··· C(24) = 3.669 Å in **GS(1Br)**; Pd ··· C(14) = 3.512 Å and Pd ··· C(24) = 3.643 Å in **TS(1Br)**).

The intermediate, **Int(1Br)**, has a mirror plane of symmetry and a dome-shaped instead of an envelope-shaped pincer (Fig. 3). The two methyl groups then lie on the same side of the molecular plane. All bonds to Pd are longer than in **GS(1Br)**, a possible consequence of the dome shape of the pincer (Table 5). The coordination around Pd is no longer purely square planar since the angles between the two transoid ligands, C(11)–Pd–C(21) and C(6)–Pd–Br, are about 156°.

The structural features for the three extrema are similar for all halides (Table 5). The Pd–C(6) bond length is minimally sensitive to the nature of the halide in **GS(1X)**, but more so for the transition state **TS(1X)** and the intermediate **Int(1X)** (Table 5).

The camel-shaped energy profile (Scheme 1) shows that the process goes *via* a double humped pathway with two transition

Table 5 Selected bond distance (Å), angles and dihedral angles (degrees) for the calculated complexes involved in the two-step fluxional process for [{CCC}PdX] and [{CNC}PdX]$^+$ (X = Cl, Br, I)

	X = Cl			X = Br			X = I		
	GS(1Cl)	**TS(1Cl)**	**Int(1Cl)**	**GS(1Br)**	**TS(1Br)**	**Int(1Br)**	**GS(1I)**	**TS(1I)**	**Int(1I)**
Pd–X	2.428	2.449	2.445	2.558	2.595	2.581	2.742	2.783	2.774
Pd–C(6)	2.015	2.048	2.055	2.018	2.049	2.060	2.020	2.056	2.065
Pd–C(11)	2.034	2.016	2.042	2.035	2.012	2.037	2.034	2.015	2.034
Pd–C(21)	2.034	2.067	2.042	2.035	2.067	2.040	2.034	2.055	2.034
C(6)–Pd–X	180.0	158.9	159.4	180.0	154.9	156.2	180.0	151.6	151.6
C(11)–Pd–C(21)	173.2	159.6	157.3	172.2	159.6	156.5	171.5	158.7	156.0
C(6)–C(1)–C(7)–N(1)	−52.2	−54.8	−49.6	−52.7	−54.9	−50.5	−52.9	−55.1	−49.2
C(6)–C(5)–C(8)–N(3)	−52.2	33.2	49.7	−52.7	27.6	49.1	−52.9	27.2	49.2
	GS(2Cl)	**TS(2Cl)**	**Int(2Cl)**	**GS(2Br)**	**TS(2Br)**	**Int(2Br)**	**GS(2I)**	**TS(2I)**	**Int(2I)**
Pd–X	2.294	2.300	2.308	2.422	2.436	2.437	2.607	2.630	2.626
Pd–N(5)	2.081	2.159	2.174	2.093	2.167	2.193	2.104	2.182	2.226
Pd–C(11)	2.031	2.029	2.046	2.034	2.021	2.046	2.037	2.013	2.035
Pd–C(21)	2.031	2.064	2.046	2.034	2.068	2.037	2.037	2.067	2.035
N(5)–Pd-X	180.0	162.3	158.6	180.0	158.8	155.1	180.0	153.5	147.9
C(11)–Pd–C(21)	175.8	163.6	161.0	174.9	163.8	161.1	173.8	164.1	160.8
N(5)–C(1)–C(7)–N(1)	−55.9	−66.5	−61.3	−56.4	−67.2	−61.2	−56.9	−66.4	−60.9
N(5)–C(5)–C(8)–N(3)	−55.9	50.9	61.3	−56.4	43.6	61.7	−56.9	33.2	60.9

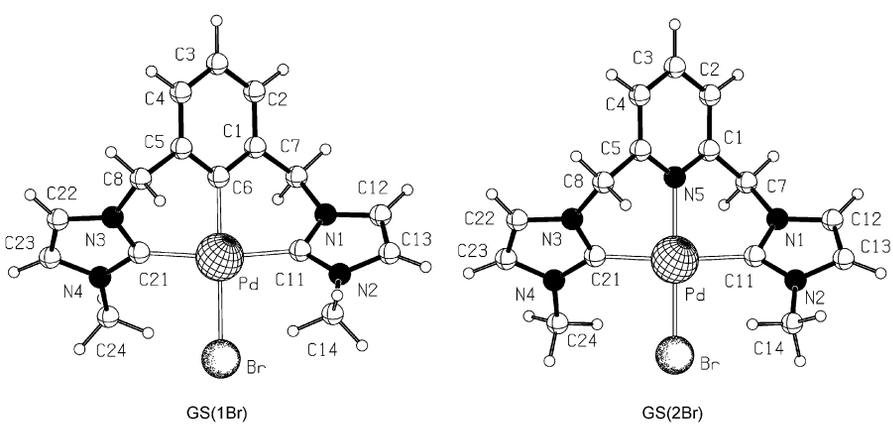

Fig. 2 Optimized geometry for Pd{CCC}Br, **GS(1Br)**, and Pd{CNC}Br$^+$, **GS(2Br)**, at the B3PW91 level.

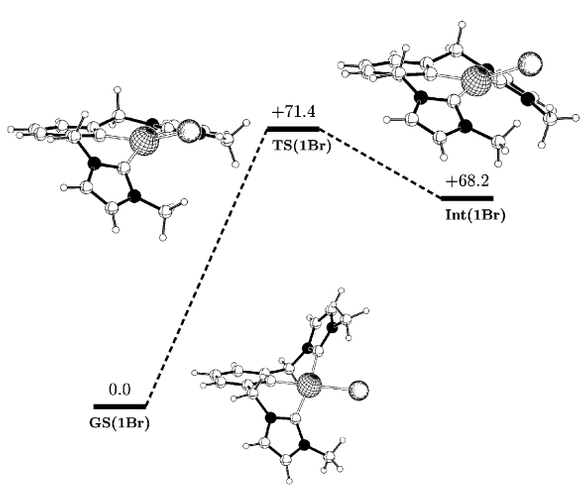

Fig. 3 Mechanism for interconversion for Pd{CCC}Br. Energies are in kJ mol^{-1}.

states, the diagram having a mirror plane of symmetry. The activation energy ($\Delta E^{\dagger}$) of the transition state **TS(1Br)** is calculated to be 71.4 kJ mol^{-1} above **GS(1Br)** which compares well with experiment ($\Delta G^{\dagger}$ = 70.9 kJ mol^{-1}). The intermediate **Int(1Br)** lies only 3.2 kJ mol^{-1} below **TS(1Br)**. This intermediate cannot be trapped and is too high in energy to affect the

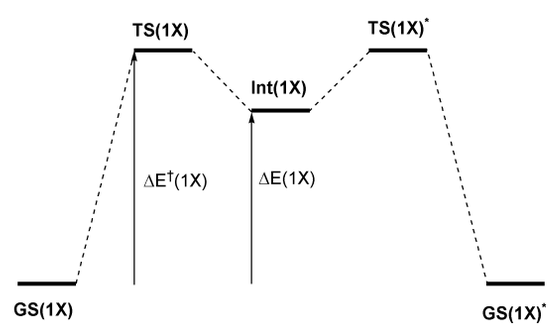

Scheme 1

NMR data. Changing the inner sphere halide X_{IS} makes very little difference to the calculated activation energies. Both the activation energy (Table 6) and the distortions in the intermediate **Int(1X)** and the transition states **TS(1X)** increases very slightly with heavier halides (Table 5). For the three halides, the intermediate is close in energy to the TS (Table 6). The influence of the solvent ($CHCl_3$) has been considered through computation of the energy on the B3PW91 optimized geometries within the PCM continuum model and has been found to have very little effect on the energy pattern (Table 6). The good agreement between the calculated and experimental barriers suggest that the calculation has properly identified the reaction path.

Table 6 Activation energy and relative energy (kJ mol^{-1}) of the intermediate for the two-step fluxional process for [{CCC}PdX] and [{CNC}PdX]$^+$ (X = Cl, Br, I). See Scheme 1 for definition of $\Delta E^\dagger$ and ΔE. GP stands for Gas Phase calculations at the B3PW91 model and PCM corresponds to calculations with a continuum model for the solvent on the B3PW91 optimized geometries

	[{CCC}PdX]				[{CNC}PdX]$^+$			
	$\Delta E^\dagger$		ΔE		$\Delta E^\dagger$		ΔE	
	GP	PCM	GP	PCM	GP	PCM	GP	PCM
X = Cl	69.9	69.5	68.0	68.9	73.2	75.5	74.9	71.8
X = Br	71.4	72.3	68.2	71.2	73.0	75.3	72.3	66.6
X = I	72.5	72.4	69.0	66.5	72.9	79.3	69.7	67.2

b) The [{CNC}PdX$_{IS}$](X$_{OS}$) systems 2. We have first calculated the dication [{CNC}Pd]$^{2+}$, **GS(2□)**, which has neither an inner nor an outer sphere anion. The activation energy for the fluxional process that interconverts hydrogen atoms on C(7) and C(8) is 47.8 kJ mol^{-1} which is significantly lower than the experimental $\Delta G^\dagger$ value of 68.5 kJ mol^{-1}. The transition state, **TS(2□)**, has a mirror plane of symmetry, a dome shaped pincer and the two methyl groups almost coplanar with the pincer plane (Fig. 4). It closely resembles the structure of the intermediate **Int(1X)** with the exception of the position of the Me groups. The camel-shaped double-humped potential energy surface (PES) has turned into a one hump situation. This illustrates the key steric role of the inner sphere halide in controlling the shape of the potential energy surface. In absence of the halide the adventitious presence of water in this site can play a decisive role. We have thus characterized the interconversion pathway for [{CNC}Pd(OH$_2$)]$^+$ and found a two-step process similar to that obtained for **GS(1Br)** with ground state **GS(2OH$_2$)**, transition state **TS(2OH$_2$)**, and intermediate **Int(2OH$_2$)**. The calculated activation energy is now 69.1 kJ mol^{-1} with an intermediate 1.5 kJ mol^{-1} below the transition state. These values are close to the experimental ones (68.5 kJ mol^{-1}). This indicates that this mechanism for fluxionality probably operates in the case of the dication and thus suggests that the cation is not free from coordinated adventitious water as indicated by the experimental work (Table 1).

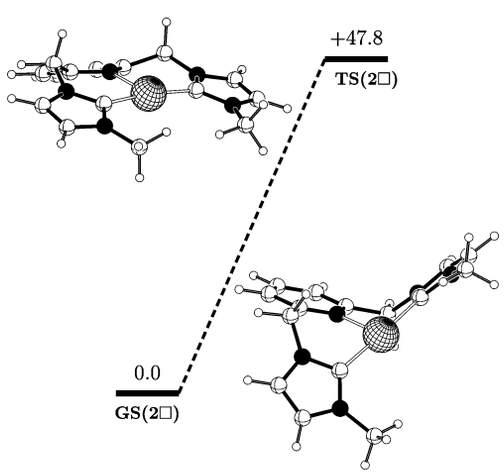

Fig. 4 Mechanism for interconversion for Pd{CNC}$^{2+}$. Energies are in kJ mol^{-1}.

The previous results show a fluxional process that is rather insensitive to the nature of the ligands since it gives similar barriers for two types of pincers and for anionic and neutral ligand X$_{IS}$ (Tables 5 and 6). In accord with this, for systems [{CNC}PdX$_{IS}$](X$_{OS}$), the calculations for fluxionality within the isolated [{CNC}PdX$_{IS}$]$^+$ cation give a barrier similar to that for the CCC pincer (Table 6). The experimental barriers (Table 1, entries 2, 4 and 6) are significantly lower than those calculated for the camel pathway thus suggesting a different mechanism operates.

The marked dependence on the outer sphere (X$_{OS}$) halide indicates that the latter is involved in the mechanism. We propose that the most likely path involves coordination of the X$_{OS}$ halide to give a five coordinate species typical for associative substitution in which the X$_{OS}$ halide has attacked the Pd atom to yield a neutral square pyramidal species, **GS(2X$_2$)**, with a long Pd–N(5) bond distance (Table 7).

Decoordination of pyridine from the pentacoordinated system goes *via* a transition state **TS(2X$_2$)** which is found 10.3 kJ mol^{-1} above **GS(2X$_2$)** and leads to a square planar intermediate with C_s symmetry (Fig. 5, X = Br). Similar energy barriers are calculated for X = Cl and I (Table 8). This square planar d^8 Pd intermediate **Int(2X$_2$)** is more stable than the square pyramidal system **GS(2X$_2$)** but the energy difference is small because the pyridine is barely bound in **GS(2X$_2$)** (Table 7).

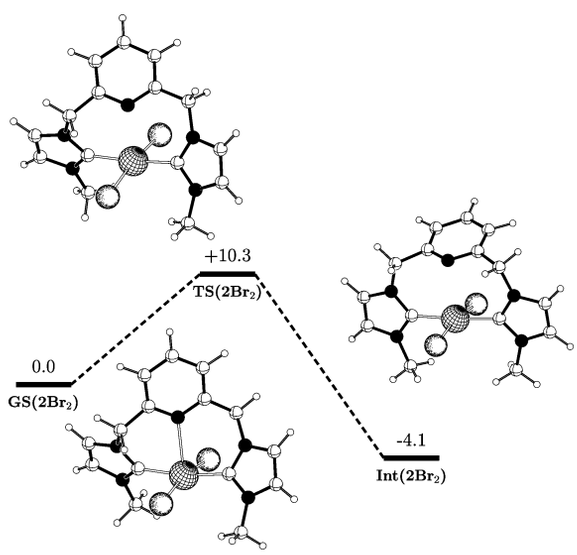

Fig. 5 Mechanism for interconversion for [Pd{CNC}(Br)$_2$]. Energies are in kJ mol^{-1}.

Inclusion of the solvent through PCM calculations does not change the energy pattern (Table 8). We also computed the energy difference between the charge separated system **GS(2X)** + X$^-$ and the neutral one **GS(2X$_2$)** with PCM calculations and the neutral system is always more stable (12.6 kJ mol^{-1}, X = Cl; 18.1 kJ mol^{-1}, X = Br; 30.7 kJ mol^{-1}, X = I). This would in principle indicate that neutral complexes **GS(2X$_2$)** should be observed experimentally, which is not the case. However entropy factors, and particularly translational entropy,[13] favour the separated system **GS(2X)** + X$^-$ by *ca.* 40 kJ mol^{-1} at 298 K, thus compensating the energy difference.

The conformer interconversion of the [{CNC}Pd(X$_{IS}$)]X$_{OS}$ complex is found to be a two-step process as for the CCC case but the two steps are very different for the two systems. In the CCC complex, the two steps involve an intramolecular structural rearrangement with no change of the metal coordination number. In the CNC case, the first step is the addition of the halide to the pyridine bound square planar cation to form a

Table 7 Selected bond distance (Å), angles and dihedral angles (degrees) for the calculated complexes involved in the two-step fluxional process for [{CNC}PdX_2] (X = Cl, Br, I)

	X = Cl			X = Br			X = I		
	GS($2Cl_2$)	**TS($2Cl_2$)**	**Int($2Cl_2$)**	**GS($2Br_2$)**	**TS($2Br_2$)**	**Int($2Br_2$)**	**GS($2I_2$)**	**TS($2I_2$)**	**Int($2I_2$)**
Pd–X	2.390	2.367	2.370	2.531	2.503	2.505	2.730	2.695	2.695
Pd–N(5)	2.578	2.657	2.753	2.554	2.635	2.735	2.525	2.605	2.713
Pd–C(11)	2.015	2.016	2.023	2.015	2.015	2.021	2.017	2.016	2.022
Pd–C(21)	2.023	2.021	2.022	2.020	2.020	2.021	2.018	2.018	2.022
N(5)–Pd–X	94.4	93.9	99.0	96.3	94.2	99.3	98.7	94.9	100.2
N(5)–Pd–C(11)	85.4	90.7	88.1	85.3	90.5	88.3	86.0	90.5	88.5
C(11)–Pd–C(21)	168.6	172.0	175.4	169.9	172.3	176.1	171.9	173.2	176.5
N(5)–C(1)–C(7)–N(1)	−63.1	−94.4	−93.1	−56.9	−91.3	−92.3	−53.2	−87.4	−90.7
N(5)–C(5)–C(8)–N(3)	−47.0	31.1	93.2	−51.6	24.8	92.3	−53.0	19.2	90.7

Table 8 Activation energy and relative energy (kJ mol^{-1}) of the intermediate for the two-step fluxional process [{CNC}PdX_2] (X = Cl, Br, I). See Scheme 1 for definition of $\Delta E^{\dagger}$ and ΔE. GP stands for Gas Phase calculations at the B3PW91 model and PCM corresponds to calculation with a continuum model for the solvent on the B3PW91 optimized geometries

	$\Delta E^{\dagger}$		ΔE	
	GP	PCM	GP	PCM
X = Cl	11.2	10.4	0.2	0.8
X = Br	10.3	11.9	−4.1	−1.4
X = I	10.1	12.8	−8.0	−3.0

pentacoordinate neutral complex. The second step corresponds to the decoordination of pyridine. The CH_2 H atoms become equivalent in this last step which is computed to have almost no barrier. We therefore propose the activation barrier observed experimentally is associated with the substitution process of X_{OS} attack on Pd. Despite numerous attempts we have not been able to locate the corresponding transition state on the potential energy surface.

In experiments designed to look at the influence of excess halide, we only saw a small increase in the barrier, probably because the polarity of the solvent has little direct consequence on a fluxional process occurring within a [{CNC}PdX_{IS}]X_{OS} tight ion pair.

Conclusions

This study shows that different mechanisms may be involved in the conformer interchange of closely related complexes. In the absence of an outer sphere anion (**1**) or with a weakly nucleophilic counterion (**2**, X = OTs), the fluxional process is intramolecular and involves the ligand without changing the coordination number of the metal centre. The strong dependence on the outer sphere anion together with the good agreement between experimental and calculated barriers lead us to propose substitution by the outer sphere anion as the slow step that triggers ligand fluxionality; we know of no prior example of such behaviour. Our observations are potentially relevant for catalysis in that the pyridine group of a CNC pincer of the type discussed here can in principle decoordinate, leading to the opening up during catalysis of an additional site that would otherwise not be considered possible. This study illustrates the key role of the counterion in the chemistry of ionic species.

Experimental

Computational details

All calculations were performed with the Gaussian 98 set of programs[14] within the framework of hybrid DFT (B3PW91)[15] on the real experimental systems. The palladium atom was represented by the relativistic effective core potential (RECP) from the Stuttgart group (17 valence electrons) and its associated (8s7p5d)/[6s5p3d] basis set,[16] augmented by an f polarization function (α = 1.472).[17] The halide atoms were also treated with Stuttgart's RECPs and the associated basis set,[18] augmented by a polarization d function (α = 0.640, Cl; α = 0.428, Br; α = 0.289, I).[19] A 6-31G(d,p) basis set[20] was used for the atoms directly bound to Pd (N and C). The remaining atoms were treated by a 6-31G basis set.[21] Full optimizations of geometry without any constraint were performed, followed by analytical computation of the Hessian matrix to confirm the nature of the located extrema as minima on the potential energy surface. The solvent effect was calculated with the PCM model[22] on the gas-phase optimized geometries.

General

All reagents are commercially available and were used as received. NMR spectra were recorded at 25 °C or at variable temperatures on Bruker spectrometers at 400 or 500 MHz (^{1}H NMR) and 100 or 125 MHz (^{13}C NMR), respectively and referenced to $SiMe_4$ (δ in ppm, J in Hz). Assignments are based either on distortionless enhancement of polarization transfer (DEPT) experiments or on homo- and heteronuclear shift correlation spectroscopy. Melting points are uncorrected. Elemental analyses were performed by Atlantic Microlab, Inc. (Norcross, GA); residual solvent molecules were identified by ^{1}H NMR.

Structure determination and refinement of [{CNC}Pd(C_5H_4N)][BF_4]$_2$

Crystals were obtained by slow diffusion of diethyl ether into a methanol solution of complex [{CNC}Pd(C_5H_4N)][BF_4]$_2$. Data were collected on a Nonius KappaCCD (Mo-K_α radiation) and corrected for absorption (SORTAV).[23] The structure was solved by direct methods (SIR92)[24] and refinement on F was carried out for all reflections. Non-hydrogen atoms were refined with anisotropic displacement parameters. Hydrogen atoms were included at calculated positions. The pertinent crystallographic data together with the refinement details are summarized in Table 3.

CCDC reference number 191341.

See http://www.rsc.org/suppdata/dt/b2/b210784h/ for crystallographic data in CIF or other electronic format.

(η^3-*C*,*C*′,*N*)(2,6-Bis{[*N*-methyl-*N*′-methylene]imidazol-2-ylidene}pyridine)chloropalladium(II)(1+) chloride, [{CNC}PdCl]Cl. The ligand synthesis was accomplished by dissolving 2,6-bis(chloromethyl)pyridine (0.3614 g, 2.053 mmol) and 1-methylimidazole (0.7725 g, 9.408 mmol) in degassed 1,4-dioxane (26 mL). This solution was refluxed at 100 °C for 13 h. After cooling, the white solid formed was collected *via* vacuum filtration and washed with 1,4-dioxane (3 × 30 mL) and then

with diethyl ether (4 × 40 mL). Yield: 0.55 g (79%). ^{1}H NMR (DMSO-d_6): δ 9.38 (s, 2H, NCHN), 7.97 (t, 1H, ^3J HH = 8.0 Hz, py-H), 7.66 (d, ^3J = 11.3, 2H, py-H), 7.63 (s, 2H, im-H), 7.41 (d, 2H, ^3J = 6.6 Hz, py-H), 5.58 (d, 4H, ^2J = 19 Hz, pyCH_2N), 3.93 (s, 6H, NCH_3). ^{13}C{^{1}H} NMR: δ 153.63 (N*C*HN), 138.76 (C_{para}). 137.33 (C_{ortho}), 123.33 (C_{im}), 123.07 (C_{im}), 122.04 (C_{meta}), 52.47 (pyCH_2N), 35.84 (NCH_3).

The resulting [{CNC}$^{2+}$2Cl$^-$] (0.3410 g, 1.002 mmol) salt and $Pd(OAc)_2$ (0.2193 g, 0.9769 mmol) were stirred in degassed DMSO (5.0 mL) for 3 h at 25 °C, then at 50 °C for 14 h, and finally for 1 h at 150 °C. The mixture was subsequently diluted with CH_2Cl_2 (25 mL) and Et_2O (150 mL). The resulting precipitate was collected, dissolved in $CHCl_3$ (40 mL) and reprecipitated with Et_2O. The precipitate, being sticky, was hard to collect, but after dissolution in $CHCl_3$, it could be transferred to a flask and isolated by removing solvent under reduced pressure. Yield 0.29 g (67%). The powder was very hydroscopic and rapidly became sticky when exposed to air. ^{1}H NMR (DMSO-d_6): δ 8.21 (t, 1H, ^3J HH = 7.7, py-H), 7.87 (d, 2H, ^3J HH = 7.6, py-H), 7.61 (s, 2H, im-H), 7.36 (s, 2H, im-H), 5.72 (s, 4H, pyCH_2N), 3.93 (s, 6H, NCH_3). ^{13}C{^{1}H} NMR: δ 164.31 (C-Pd), 155.47 (C_{ortho}), 141.67 (C_{para}), 125.57 (C_{meta}), 123.49 (im-C), 121.55 (im-C), 54.32 (pyCH_2N), 36.97 (NCH_3). Anal. Calcd. for $C_{15}H_{17}N_5Cl_2Pd_1 \cdot 1H_2O$: C, 38.94, H, 4.14, N, 15.14. Found: C, 39.06, H, 4.26, N, 15.06%. Mp: 235–239 °C (decomp.).

(η^3-*C*,*C*′,*N*)(2,6-Bis{[*N*-methyl-*N*′-methylene]imidazol-2-ylidene}pyridine)aquapalladium(II)(2+) fluoroborate, [{CNC}Pd-(OH_2)]BF_4. A solution of [{CNC}PdCl]Cl (0.215 g, 0.484 mmol) and $AgBF_4$ (0.199 g 1.02 mmol) was stirred in acetone in the dark for 16 h. The resulting solution was then filtered over Celite (2 times) and the filtrate evaporated under reduced pressure. Yield: 0.306 g. The product was recrystallized from acetone/Et_2O. ^{1}H NMR (DMSO-d_6): δ 8.21 ((t, 1H, ^3J = 7.9 Hz, py-H), 7.84 (d, 2H, ^3J = 7.7 Hz, py-H), 7.63 (s, 2H, im-H), 7.43 (s, 2H, im-H), 5.77 (d, 2H, ^2J = 15.1 Hz, py-CH_2N), 5.59 (d, 2H, ^2J = 10.5 Hz, py-CH_2N), 3.94 (s, 6H, NCH_3), 3.35 (water in DMSO), 2.50 (DMSO), 2.08 (acetone). ^{13}C{^{1}H} NMR: δ 206.31 (acetone), 162.64 (C-Pd), 156.34 (C_{ortho}), 142.26 (C_{para}), 125.97 (C_{meta}), 123.75 (im-C), 122.15 (im-C), 54.40 (pyCH_2N), 39.52 (DMSO), 36.72 (NCH_3), 30.56 (acetone). Anal. Calcd. for $C_{15}H_{19}B_2F_8N_5OPd$ (565.37)·C_3H_6O: C: 34.68, H: 4.04, N: 11.23,. Found: C: 34.67, H: 3.81, N: 11.68%. Mp: 207–212 °C (decomp.)

(η^3-*C*,*C*′,*N*)(2,6-Bis{[*N*-methyl-*N*′-methylene]imidazol-2-ylidene}pyridine)iodopalladium(II)(1+) iodide, [{CNC}PdI]I. A solution of [{CNC}Pd(solvent)]$(BF_4)_2$ (0.1168 g, 0.2066 mmol) and NaI (0.3417 g, 2.279 mmol) was stirred in acetone for 16 h. The resulting solution was filtered and the solvent was evaporated under reduced pressure. The resulting residue was redissolved in $CHCl_3$ and filtered again; the solvent was then evaporated under reduced pressure to give a light yellow solid that was then dried *in vacuo*. Yield: 0.127g, (98%). The product was recrystallized by dissolving in boiling EtOH, slow cooling to 25 °C, then storing at −20 °C for 10 d. ^{1}H NMR (DMSO-d_6): δ 8.21 (t, 1H, ^3J = 3.9 Hz, py-H), 7.87 (d, 2H, ^3J = 7.7 Hz, py-H), 7.61 (s, 2H, im-H), 7.40 (s, 2H, im-H), 5.67 (s, 4H, pyCH_2N), 3.93 (s, 6H, NCH_3). ^{13}C{^{1}H} NMR: δ 164.34 (C-Pd), 154.57 (C_{ortho}), 141.61 (C_{para}), 124.89 (C_{meta}), 123.52 (im-C), 122.10 (im-C), 54.38 (pyCH_2N), 38.84 (NCH_3). Anal Calcd. $C_{15}H_{17}I_2N_5Pd$ (627.56)·0.5EtOH: C: 29.54, H: 3.10, N: 10.76. Found: C: 29.14, H: 2.94, N: 10.67%. Mp: 235–240 °C (decomp.).

(η^3-*C*,*C*′,*N*)(2,6-Bis{[*N*-methyl-*N*′-methylene]imidazol-2-ylidene}pyridine)chloropalladium(II)(1+) tosylate, [{CNC}Pd-Cl]OTs. A solution of [{CNC}PdCl]Cl (0.198 g, 0.4452 mmol) and NaOTs (0.0868 g, 0.4470 mmol) was stirred in CH_2Cl_2 (150 mL) for 2 d. The resulting solution was then filtered through Celite and the solvent was evaporated under reduced pressure. The solid was dried overnight *in vacuo*. Yield: 0.236 g (91%). The product could be recrystallized from CH_2Cl_2/Et_2O. ^{1}H NMR (DMSO-d_6): δ 8.20 (t, 1H, ^3J = 7.7 Hz, py-H), 7.84 (d, 2H, ^3J = 7.7 Hz, py-H), 7.58 (d, 2H, ^3J = 1.6 Hz, im-H), 7.46 (d, 2H, ^3J = 8.0 Hz, tosylate-H), 7.36 (d, 2H, ^3J = 1.6 Hz, im-H), 7.10 (d, 2H, ^3J = 7.9 Hz, tosylate-H), 5.70 (d, 4H, ^2J = 9.6 Hz, py-CH_2-N), 3.93 (s, 6H, NCH_3), 2.28 (s, 3H, CH_3). ^{13}C{^{1}H} NMR: δ 164.22 (C-Pd), 155.38 (C_{ortho}), 145.72 (C–S), 141.66 (C_{para}), 137.46 (*C*-CH_3), 127.96 (S-C-(*C*H)$_2$), 125.51 (C_{meta}), 125.39 (H_3C-C-(*C*H)$_2$), 123.48 (im-C), 121.50 (im-C), 54.32 (pyCH_2N), 36.91 (NCH_3), 20.70 (*C*H_3-C). Anal. Calcd. $C_{22}H_{24}ClN_5O_3PdS$ (580.40)·0.33CH_2Cl_2: C: 44.07, H: 4.08, N: 11.51, Cl: 9.71. Found: C: 43.76, H: 4.24, N: 11.06, Cl: 9.73%. Mp: 219–225 °C (decomp.).

(η^3-*C*,*C*′,*N*)(2,6-Bis{[*N*-methyl-*N*′-methylene]imidazol-2-ylidene}pyridine)bromopalladium(II)(1+) tosylate, [{CNC}Pd-Br]OTs. A solution of [{CNC}PdBr]Br[1] (0.096 g, 0.180 mmol) and AgOTs (0.0523 g, 0.187 mmol) was stirred in methanol (150 mL) for 20 h. The resulting solution was filtered through Celite and the solvent evaporated under reduced pressure. The yellow solid was dried overnight *in vacuo*. Yield: 0.091 g (81%). ^{1}H NMR (DMSO-d_6): δ 8.21 (t, 1H, ^3J = 8.7 Hz py-H), 7.85 (d, 2H, ^3J = 7.8 Hz, py-H), 7.59 (d, 2H, ^3J = 1.6 Hz, im-H), 7.47 (d, 2H, ^3J = 8.1 Hz, tosylate-H), 7.36 (d, 2H, ^3J = 1.6 Hz, im-H), 7.11 (d, 2H, ^3J = 7.1 Hz, tosylate-H), 5.67 (d, 4H, ^2J = 8.6 Hz, py-CH_2-N), 4.07 (s, 6H, NCH_3), 2.28 (s, 3H, CH_3). ^{13}C{^{1}H} NMR: δ 164.26 (C-Pd), 155.26 (C_{ortho}), 145.75 (*C*-S), 141.78 (C_{para}), 137.64 (*C*-CH_3), 128.09 (S-C-(*C*H)$_2$), 125.51 (H_3C-C-(*C*H)$_2$), 125.44 (C_{meta}), 123.66 (im-C), 121.62 (im-C), 54.50 (pyCH_2N), 38.08 (NCH_3), 20.81 (*C*H_3-C). Anal. Calcd. $C_{22}H_{24}BrN_5O_3PdS$·CH_3OH (671.85): C: 42.05, H: 4.30, N: 10.66, Br: 12.16. Found: C: 42.25, H: 4.08, N: 10.72, Br: 12.13%. Mp: 215–219 °C (decomp.).

(η^3-*C*,*C*′,*N*)(2,6-Bis{[*N*-methyl-*N*′-methylene]imidazol-2-ylidene}pyridine)iodopalladium(II)(1+) tosylate, [{CNC}PdI]OTs. A solution of [{CNC}PdI]I (0.0581 g, 0.0926 mmol) and AgOTs (0.0272 g, 0.0975 mmol) was stirred in methanol (150 mL) for 2 d. The resulting solution was then filtered through Celite and the solvent was evaporated under reduced pressure. The solid was dried overnight *in vacuo*. Yield: 0.058 g (93%). The product could be recrystallized from acetone/Et_2O. ^{1}H NMR (DMSO-d_6): δ 8.20 (t, 1H, ^3J = 7.7 Hz, py-H), 7.84 (d, 2H, ^3J = 7.7 Hz, py-H), 7.59 (d, 2H, ^3J = 1.6 Hz, im-H), 7.46 (d, 2H, ^3J = 8.0 Hz, tosylate-H), 7.36 (d, 2H, ^3J = 1.6 Hz, im-H), 7.10 (d, 2H, ^3J = 7.9 Hz, tosylate-H), 5.66 (d, 4H, ^2J = 5.0 Hz, py-CH_2-N), 3.93 (s, 6H, NCH_3), 2.28 (s, 3H, CH_3). ^{13}C{^{1}H} NMR: δ 164.88 (C-Pd), 155.11 (C_{ortho}), 146.23 (S-C), 142.12 (C_{para}), 137.86 (*C*-CH_3), 128.38 (S-C-(*C*H)$_2$), 125.94 (H_3C-C-(*C*H)$_2$), 125.43 (C_{meta}), 124.06 (im-C), 122.64 (im-C), 54.90 (pyCH_2N), 31.05 (NCH_3), 21.13 (*C*H_3-C). Anal. Calcd. $C_{22}H_{24}N_5IO_3PdS \cdot H_2O$ (671.85): C: 38.30, H: 3.80, N: 10.15, I: 18.89. Found: C: 38.58, H: 3.80, N: 9.96, I: 17.58%. Mp: 195–198 °C (decomp.).

(η^3-*C*,*C*′,*N*)(2,6-Bis{[*N*-methyl-*N*′-methylene]imidazol-2-ylidene}pyridine)pyridinepalladium(II)(2+) fluoroborate, [{CNC}-Pd(C_5H_5N)]$(BF_4)_2$. A solution of [{CNC′}PdBr]Br (0.191g, 0.356 mmol) and $AgBF_4$ (0.1515 g, 0.7782 mmol) was stirred in acetone (15 mL) and pyridine (1.50 mL, 18.5 mmol) for 20 h. The resulting solution was then filtered through Celite and the solvent was evaporated under reduced pressure. The resulting oil was isolated from methanol/Et_2O. Yield: 0.219 g (95%). The product was recrystallized from methanol/Et_2O. ^{1}H NMR (DMSO-d_6): δ 8.94 (d, 2H, ^3J = 4.7 Hz, py-H) 8.22 (m, 2H, py-H), 7.85 (d, 2H, ^3J = 7.7 Hz, py-H), 7.74 (m, 2H, py-H), 7.62 (d, 2H, ^3J = 1.6 Hz, im-H), 7.29 (d, 2H, ^3J = 1.6 Hz, im-H), 6.02 (d, 2H, ^2J = 14.9 Hz, py-CH_2-N), 5.68 (d, 2H, ^2J = 15.0 Hz, py-CH_2-N), 2.99 (s, 6H, NCH_3), ^{13}C{^{1}H} NMR: δ 165.05,

(C-Pd), 156.21 (C_{ortho}), 154.45 (py-C_{ortho}) 142.73 (C_{para}), 141.14 (py-C_{para}), 127.66 (py-C_{meta}), 126.36 (C_{meta}), 124.04 (im-C), 122.17 (im-C), 54.68 ($pyCH_2N$), 35.67 (NCH_3). Anal. Calcd. $C_{20}H_{22}N_6B_2F_8Pd$ (626.46)·H_2O: C: 37.27, H: 3.75, N: 13.04. Found: C: 37.31, H: 3.53, N: 12.67%. Mp: 290–300 °C (decomp.).

(η³-*C*,*C*′,*N*)(2,6-Bis{[*N*-methyl-*N*′-methylene]imidazol-2-ylidene}pyridine)bromopalladium(II)(1+) bromide, [{CNC}Pd-Br]Br. [{CNC′}$^{2+}$2Br$^-$] was synthesized from 2,6-bis(bromomethyl)pyridine (3.0 g, 11.34 mmol) and 1-butylimidazole (4.5 mL, 34.2 mmol) in 1,4-dioxane (100 mL). The reaction mixture was heated to 100 °C for 12 hours during which a yellow oil separated. After cooling to 20 °C, the 1,4-dioxane was decanted and the precipitate recrystallized three times from $CHCl_3$ (20 mL)/Et_2O (200 mL). Prolonged drying *in vacuo* gave 4.79 g (82%) of an off-white solid. The product was very hydroscopic and was used in the next step without further purification. ^{1}H NMR (DMSO-d_6): δ 9.36 (s, 2H, NHCN), 7.98 (t, 1H, ^3J = 7.6 Hz, py-H), 7.86 (s, 2H, im-H), 7.75 (d, 2H, im-H), 7.48 (d, 2H, ^3J = 7.6 Hz, py-H), 5.57 (s, 4H, py-CH_2), 4.24 (t, 4H, ^3J = 7.3 Hz, $NCH_2CH_2CH_2CH_3$), 1.79 (quintet, 4H, ^3J = 7.3 Hz, $NCH_2CH_2CH_2CH_3$), 1.27 (sextet, 4H, ^3J = 7.6 Hz, $NCH_2CH_2CH_2CH_3$), 0.91 (t, 6H, ^3J = 7.3 Hz, $NCH_2CH_2CH_2CH_3$). ^{13}C{^{1}H} NMR: δ 153.64 (C_{ortho}), 138.86 (C_{para}), 136.71 (NCHN), 123.23 (im-C), 122.21 (im-C), 122.13 (C_{meta}), 52.62 (py-CH_2), 48.61 ($NCH_2CH_2CH_2CH_3$), 31.73 ($NCH_2CH_2CH_2CH_3$), 19.15 ($NCH_2CH_2CH_2CH_3$), 13.68 ($NCH_2CH_2CH_2CH_3$).

[{CNC′}$^{2+}$2Br$^-$] (1.16 g, 2.25 mmol) and $Pd(OAc)_2$ (0.500 g, 2.23 mmol) were dissolved in degassed DMSO (10.0 mL), and stirred for 3 h at 25 °C, then at 50 °C for 12 h, and finally for 1 h at 160 °C. After cooling to 20 °C, the reaction mixture was filtered. The filtrate was dissolved in CH_2Cl_2 (50 mL) and isolated with Et_2O (200 mL); the supernatant was decanted. The procedure was repeated three times to give 1.176 g (85%) of the crude product as a yellowish solid. Analytically pure material was obtained by recrystallization from CH_2Cl_2/pentane (2×). ^{1}H NMR (DMSO-d_6): δ 8.21 (t, 1H, ^3J = 7.7 Hz, py-H), 7.85 (d, 2H, ^3J = 7.7 Hz, py-H), 7.59 (d, 2H, ^3J = 1.8 Hz, im-H), 7.44 (d, 2H, ^3J = 1.8 Hz, im-H), 5.64 (br m, 4H, py-CH_2), 4.49 (br s, 2H, $NCHCH_2CH_2CH_3$), 4.26 (br, s, $NCHCH_2CH_2CH_3$) 1.79 (quintet, 4H, ^3J = 7.6 Hz, $NCH_2CH_2CH_2CH_3$), 1.24 (sextet, 4H, ^3J = 7.6 Hz, $NCH_2CH_2CH_2CH_3$), 0.89 (t, 6H, ^3J = 7.5 Hz, $NCH_2CH_2CH_2CH_3$). ^{13}C{^{1}H} NMR: δ 163.99 (C-Pd), 155.19 (C_{ortho}), 141.83 (C_{para}), 122.22 (im-C), 122.03 (im-C), 125.41 (C_{meta}), 54.44 (py-CH_2), 48.65 ($NCH_2CH_2CH_2CH_3$), 32.90 ($NCH_2CH_2CH_2CH_3$),18.95($NCH_2CH_2CH_2CH_3$),13.52($NCH_2CH_2CH_2CH_3$). Anal. Calcd. for $C_{21}H_{29}Br_2N_5Pd$ (617.72): C: 40.83, H: 4.73, N: 11.34. Found: C: 40.96, H: 4.78, N: 11.32%. Mp: 257–262 °C (decomp.).

Acknowledgements

We gratefully acknowledge financial support from Deutsche Akademie der Naturforscher Leopoldina (Grant BMBF-LPD 9901/8-37; S.G.) the Swiss National Foundation (M.A.), the U.S. DOE and NSF (R.H.C. and J.W.F.). We also thank the CINES (projet LSD2217) for a generous donation of computational time.

References

1 S. Gründemann, M. Albrecht, J. A. Loch, J. W. Faller and R. H. Crabtree, *Organometallics*, 2001, **20**, 5485.
2 C. Bolm, J. P. Hildebrand, K. Muniz and N. Hermanns, *Angew. Chem., Int. Ed.*, 2001, **40**, 3285.
3 For examples of bis-carbenes: (*a*) W. A. Herrmann, V. P. W. Bohm, C. W. K. Gstottmayr, M. Grosche, C.-P. Reisinger and T. Weskamp, *J. Organomet. Chem.*, 2001, **616**, 617; (*b*) R. E. Douthwaite, M. L. H. Green, P. J. Silcock and P. T. Gomes, *J. Chem. Soc., Dalton Trans.*, 2002, 1386; (*c*) A. M. Magill, D. S. McGuinness, K. J. Cavell, G. J. P. Britovsek, V. C. Gibson, A. J. P. White, D. J. Williams, A. H. White and B. W. Skelton, *J. Organomet. Chem.*, 2001, **546**, 617; (*d*) D. S. McGuinness and K. J. Cavell, *Organometallics*, 2000, **19**, 741; (*e*) C. Zhang and M. L. Trudell, *Tetrahedron Lett.*, 2000, **41**, 595; (*f*) N. J. Whitcombe, M. M. Hii and S. E. Gibson, *Tetrahedron*, 2001, **57**, 7449; for examples of tris-chelates (*g*) D. J. Nielsen, K. J. Cavell, B. W. Skelton and A. H. White, *Inorg. Chim. Acta*, 2002, **327**, 116; (*h*) A. A. D. Tulloch, A. A. Danopoulos, G. J. Tizzard, S. J. Coles, M. B. Hursthouse, R. S. Hay-Motherwell and W. B. Motherwell, *Chem. Commun.*, 2001, 1270; for examples where atropisomer interconversion must be prevented; (*i*) B. A. Markies, P. Wijkens, J. Boersma, H. Kooijman, N. Veldman, A. L. Spek and G. van Koten, *Organometallics*, 1994, **13**, 3244.
4 M. J. McGlinchey, *Can. J. Chem.*, 2001, **79**, 1295.
5 For one example: M. T. Ashby, G. N. Govindan and A. K. Grafton, *J. Am. Chem. Soc.*, 1994, **116**, 4801.
6 E. W. Abel and K. G. Orrell, NMR of Fluxional Processes, in *Encyclopaedia of Inorganic Chemistry*, R. B. King, ed. John Wiley and Sons, New York, 1994, pp. 2581–2615 and refs. cited therein.
7 J. W. Faller, Stereochemical Nonrigidity of Organometallic Complexes, in *Encyclopaedia of Inorganic Chemistry*, R. B. King, ed. John Wiley and Sons, New York, 1994, pp. 3914–3933.
8 A. Kovacevic, S. Gründemann, J. R. Miecznikowski, E. Clot, O. Eisenstein and R. H. Crabtree, *Chem. Commun.*, 2002, 2580.
9 S. Gründemann, A. Kovacevic, M. Albrecht, J. W. Faller and R. H. Crabtree, *Chem. Commun.*, 2001, 2274.
10 S. Gründemann, A. Kovacevic, M. Albrecht, J. W. Faller and R. H. Crabtree, *J. Am. Chem. Soc.*, 2002, **124**, 10473.
11 A. Macchioni, C. Zuccaccia, E. Clot, K. Gruet and R. H. Crabtree, *Organometallics*, 2001, **20**, 2367.
12 (*a*) M. Elian and R. Hoffmann, *Inorg. Chem.*, 1975, **14**, 1058; (*b*) T. A. Albright, J. K. Burdett, M.-H. Whangbo, *Orbital Interactions in Chemistry*, Wiley, New York, NY, 1985; (*c*) M. Ogasawara, S. A. Macgregor, W. E. Streib, K. Folting, O. Eisenstein and K. G. Caulton, *J. Am. Chem. Soc.*, 1996, **118**, 10189.
13 L. A. Watson and O. Eisenstein, *J. Chem. Ed.*, 2001, **79**, 1269.
14 M. J. Frisch, G. W. Trucks, H. B. Schlegel, G. E. Scuseria, M. A. Robb, J. R. Cheeseman, V. G. Zakrzewski, J. A. Montgomery, R. E. Stratmann, J. C. Burant, S. Dapprich, J. M. Millam, A. D. Daniels, K. N. Kudin, M. C. Strain, O. Farkas, J. Tomasi, V. Barone, M. Cossi, R. Cammi, B. Mennucci, C. Pomelli, C. Adamo, S. Clifford, J. Ochterski, G. A. Petersson, P. Y. Ayala, Q. Cui, K. Morokuma, D. K. Malick, A. D. Rabuck, K. Raghavachari, J. B. Foresman, J. Cioslowski, J. V. Ortiz, B. B. Stefanov, G. Liu, A. Liashenko, P. Piskorz, P. I. Komaromi, G. Gomperts, R. L. Martin, D. J. Fox, T. Keith, M. A. Al-Laham, C. Y. Peng, A. Nanayakkara, C. Gonzalez, M. Challacombe, P. M. W. Gill, B. G. Johnson, W. Chen, M. W. Wong, J. L. Andres, M. Head-Gordon, E. S. Replogle, J. A. Pople, Gaussian 98 (Rev A7), Gaussian, Inc., Pittsburgh, PA, 1998.
15 (*a*) A. D. J. Becke, *J. Chem. Phys.*, 1993, **98**, 5648; (*b*) J. P. Perdew and Y. Wang, *Phys. Rev. B*, 1992, **82**, 284.
16 D. Andrae, U. Häussermann, M. Dolg, H. Stoll and H. Preuss, *Theor. Chim. Acta*, 1990, **77**, 123.
17 A. W. Ehlers, M. Böhme, S. Dapprich, A. Gobbi, A. Höllwarth, V. Jonas, K. F. Köhler, R. Stegmann, A. Veldkamp and G. Frenking, *Chem. Phys. Lett.*, 1993, **208**, 111.
18 A. Bergner, M. Dolg, W. Küchle, H. Stoll and H. Preuss, *Mol. Phys.*, 1990, **30**, 1431.
19 A. Höllwarth, M. Böhme, S. Dapprich, A. W. Ehlers, A. Gobbi, V. Jonas, K. F. Köhler, R. Stegmann, A. Veldkamp and G. Frenking, *Chem. Phys. Lett.*, 1993, **208**, 237.
20 P. C. Hariharan and J. A. Pople, *Theor. Chim. Acta*, 1973, **28**, 213.
21 W. J. Hehre, R. Ditchfield and J. A. Pople, *J. Chem. Phys.*, 1972, **56**, 2257.
22 (*a*) S. Miertus, E. Scrocco and J. Tomasi, *Chem. Phys.*, 1981, **55**, 117; (*b*) S. Miertus and J. Tomasi, *Chem. Phys.*, 1982, **65**, 239; (*c*) M. Cossi, V. Barone, R. Cammi and J. Tomasi, *Chem. Phys. Lett.*, 1996, **255**, 327.
23 (*a*) R. H. Blessing, *Acta Crystallogr., Sect. A*, 1995, **51**, 33; (*b*) R. H. Blessing, *J. Appl. Crystallogr.*, 1997, **30**, 421.
24 A. Altomare, G. Cascarano, C. Giacovazzo and A. Guagliardi, *J. Appl. Crystallogr.*, 1993, **26**, 343.